International Communications in Heat and Mass Transfer 39 (2012) 1–7

Contents lists available at SciVerse ScienceDirect

International Communications in Heat and Mass Transfer

journal homepage: www.elsevier.com/locate/ichmt

Turbulent flow with combustion in a moving bed ☆

Marcelo J.S. de Lemos *, Ana C. Pivem

Departamento de Energia, IEME, Instituto Tecnológico de Aeronáutica, ITA, 12228-900, São José dos Campos, S.P., Brazil

ARTICLE INFO

Available online 28 September 2011

Keywords:
Combustion
Moving bed
Porous media
Turbulence

ABSTRACT

This paper presents a mathematical model for treating turbulent combusting flows in a moving porous bed, which might be useful to design and analysis of modern and advanced biomass gasification systems. Here, one explicitly considers the intra-pore levels of turbulent kinetic energy and the movement of the rigid solid matrix is considered to occur at a steady speed. Transport equations are written in their time-and-volume-averaged form and a volume-based statistical turbulence model is applied to simulate turbulence generation due to the porous matrix. The rate of fuel consumption is described by an Arrhenius expression involving the product of the fuel and oxidant mass fractions. Results indicate that fixing the gas speed and increasing the speed of the solid matrix pushes the flame front towards the end of the reactor. Also, since the rate of production of turbulence is dependent on the relative velocity between phases, as the solid velocity approaches that of the gas stream, the level of turbulence in the flow is reduced.

1. Introduction

Energy production based on biomass combustion has called the attention of the world for its potential substitution of non-renewable fossil fuels. Biomass pelletization and preparation for energy production systems may involve a moving porous bed [1–3] in which an exothermic reaction occurs. Examples of studies on such systems are given by Ryu et al. [4], Boman et al. [5] and Shimizu et al. [6] who presented mathematical models for gasification and combustion of renewable fuels. Kayal and Chakravarty [7], Rogel et al. [8] and Nussbaumer et al. [9] investigated technologies to cope with the problem of pollutant emission during combustion and co-combustion of biomass. Related investigations concerning studies on reactive flows in permeable media [10–15], including recent reviews on combustion of gases [16] and liquids [17] in the so-called porous burners, have also contributed to the modeling of flows with combustion through a permeable medium. Recent developments on free flame modeling [18, 19] will further benefit the analyses of the heterogeneous systems just reviewed. Accordingly, the ability to more realistic model such devices is of great advantage to the analysis and optimization of a number of energy, food and materials production processes.

Motivated by the foregoing, in a series of papers a general mathematical model for turbulent flow in porous media, including flows with macroscopic interfaces [20], buoyant flows [21] and impinging jets, with [22, 23] and without [24] thermal non-equilibrium, was developed and documented in a book [25]. Such model was further extended to include movement of the solid phase for non-reacting flows [26] with heat transfer [27]. Subsequently, combustion of gases within a fixed porous medium was also considered [28, 29].

The objective of this contribution is then to combine the previous separated analyses of movement of a porous bed along with an inert flow [26, 27] with that of combustion of a gaseous fuel through a fixed medium [28, 29]. By that, a more complete and more general model is investigated as solutions of a broader range of problems are sought, which aim at simulate, in a more realistic fashion, modern equipment for energy production using renewable fuels.

2. Macroscopic flow model

As mentioned, the thermo-mechanical model here employed is based on concepts already fully described in the literature [25]. In that work, transport equations are volume averaged over a Representative Elementary Volume (REV) according to the Volume Averaging Theorem [30–32]. In addition, the use of time decomposition of flow variables, followed by standard time-averaging procedure, was applied to model turbulence. As the entire equation set is already fully available in the open literature, these equations will be reproduced here and details about their derivations can be obtained in the aforementioned references. Essentially, in all the above-mentioned work, the flow variables are decomposed in a volume mean and a deviation (classical porous media analysis) in addition to being also decomposed in a time-mean and fluctuating values (classical turbulent flow treatment). As said, because mathematical details and proofs of such "double-decomposition" concept are available in a number of papers in the literature, they are not repeated here. Only final equations in their steady-state form are presented below.

☆ Communicated by W.J. Minkowycz.

* Corresponding author.
E-mail address: delemos@ita.br (M.J.S. de Lemos).

0735-1933/$ – see front matter © 2011 Elsevier Ltd. All rights reserved.
doi:10.1016/j.icheatmasstransfer.2011.09.001

Nomenclature

Latin characters

A	Pre-exponential factor
c_F	Forchheimer coefficient
c_p	Specific heat
$D=[\nabla\mathbf{u}+(\nabla\mathbf{u})^T]/2$	Deformation rate tensor
D_ℓ	Diffusion coefficient of species ℓ
D_{diff}	Macroscopic diffusion coefficient
D_{disp}	Dispersion tensor due to dispersion
$D_{disp,t}$	Dispersion tensor due to turbulene
D_{eff}	Effective dispersion
K	Permeability
k_f	Fluid thermal conductivity
k_s	Solid thermal conductivity
$\mathbf{K}_{eff}$	Effective Conductivity tensor
m_ℓ	Mass fraction of species ℓ
Pr	Prandtl number
S_{fu}	Rate of fuel consumption
T	Temperature
$\mathbf{u}$	Microscopic velocity
$\mathbf{u}_D$	Darcy or superficial velocity (volume average of $\mathbf{u}$)

Greek characters

α	Thermal diffusivity
β_r	Extinction coefficient
ΔV	Representative elementary volume
ΔV_f	Fluid volume inside ΔV
ΔH	Heat of combustion
μ	Dynamic viscosity
ν	Kinematic viscosity
ρ	Density
ϕ	$\phi = {\Delta V_f}/{\Delta V}$, Porosity
ψ	Excess air-to-fuel ratio

Special characters

φ	General variable
$\langle\varphi\rangle^i$	Intrinsic average
$\langle\varphi\rangle^v$	Volume average
$^i\varphi$	Spatial deviation
$\overline{\phi}$	Time average
ϕ'	Time fluctuation
$\|\boldsymbol{\varphi}\|$	Absolute value (Abs)
$\boldsymbol{\varphi}$	Vectorial general variable
$(\ )_{s,f}$	solid/fluid
$(\ )_{eff}$	Effective value, $\phi\varphi_f+(1-\phi)\varphi_s$
$(\ )_\phi$	Macroscopic value
$(\ )_{fu}$	Fuel
$(\ )_{ox}$	Oxygen

2.1. Macroscopic slip velocity

In order to analyze the effect of the motion of the permeable structure, one needs first to define velocities and their averages relative to a fixed representative elementary control-volume. One should point out, however, that here only cases where the solid phase velocity is kept constant will be considered.

A moving bed crosses a fixed reactor in addition to a flowing fluid, which is not necessarily moving with a velocity aligned with the solid phase velocity (Fig. 1). The steps below show first some basic definitions prior to presenting a proposal for a set of transport equations for analyzing such systems.

A general form for a volume-average of any property φ, distributed within a phase γ that occupy volume ΔV_γ, can be written as [32],

$$\langle\varphi\rangle^\gamma = \frac{1}{\Delta V_\gamma}\int_{\Delta V_\gamma}\varphi\, dV_\gamma. \tag{1}$$

In the general case, the volume ratio occupied by phase γ will be $\phi^\gamma = \Delta V_\gamma/\Delta V$.

If there are two phases, a solid ($\gamma=s$) and a fluid phase ($\gamma=f$), volume average can be established on both regions. Also,

$$\phi^s = \Delta V_s/\Delta V = 1-\Delta V_f/\Delta V = 1-\phi^f \tag{2}$$

and, for simplicity of notation, one can drop the superscript "f" to get $\phi^s = 1-\phi$. For permeable media, phi is known as porosity.

As such, calling the instantaneous local velocities for the solid and fluid phases, $\mathbf{u}_s$ and $\mathbf{u}$, respectively, one can obtain the average for the solid velocity, within the solid phase, as follows,

$$\langle\mathbf{u}\rangle^s = \frac{1}{\Delta V_s}\int_{\Delta V_s}\mathbf{u}_s\, dV_s \tag{3}$$

which, in turn, can be related to the average velocity referent to the entire REV as,

$$\mathbf{u}_S = \overbrace{\frac{\Delta V_s}{\Delta V}}^{(1-\phi)}\underbrace{\frac{1}{\Delta V_s}\int_{\Delta V_s}\mathbf{u}_s\, dV_s}_{\langle\mathbf{u}\rangle^s}. \tag{4}$$

A further approximation herein is that the porous bed is rigid and moves with a steady average velocity $\mathbf{u}_S$. Note that the condition of steadiness for the solid phase gives $\mathbf{u}_S = \bar{\mathbf{u}}_S = const$ where the overbar denotes, as usual in the literature, time-averaging.

For the fluid phase, the intrinsic (fluid) volume average gives, after using the subscript "i" also for consistency with the literature,

$$\langle\bar{\mathbf{u}}\rangle^i = \frac{1}{\Delta V_f}\int_{\Delta V_f}\bar{\mathbf{u}}\, dV_f. \tag{5}$$

On a total-volume basis, both velocities can then be written as,

$$\bar{\mathbf{u}}_D = \phi\langle\bar{\mathbf{u}}\rangle^i, \mathbf{u}_S = (1-\phi)\langle\mathbf{u}\rangle^s = const. \tag{6}$$

where, $\bar{\mathbf{u}}_D$ is the average surface velocity (also known as seepage, superficial, filter or Darcy velocity).

In the general case, $\bar{\mathbf{u}}_D$ and $\mathbf{u}_S$ need not to be aligned with each other as in the drawing of Fig. 1. For a general three-dimensional flow they are written in Cartesian coordinates as,

$$\bar{\mathbf{u}}_D = \bar{u}_D\,\hat{i} + \bar{v}_D\,\hat{j} + \bar{w}_D\,\hat{k}\,;\ \mathbf{u}_S = u_S\,\hat{i} + v_S\,\hat{j} + w_S\,\hat{k} \tag{7}$$

where u, v, and w are the Cartesian components.

A total-volume based relative velocity is defined as,

$$\bar{\mathbf{u}}_{rel} = \bar{\mathbf{u}}_D - \mathbf{u}_S. \tag{8}$$

Further,

$$\bar{\mathbf{u}}_{rel} = \phi\langle\bar{\mathbf{u}}\rangle^i - (1-\phi)\langle\mathbf{u}\rangle^s;\ \ \bar{\mathbf{u}}_{rel} = \phi\left(\langle\bar{\mathbf{u}}\rangle^i + \langle\mathbf{u}\rangle^s\right) - \langle\mathbf{u}\rangle^s. \tag{9}$$

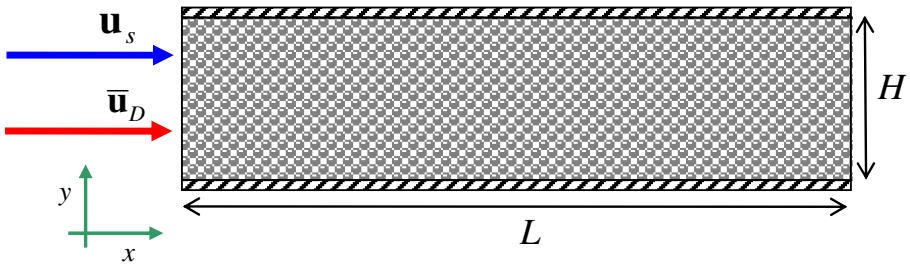

Fig. 1. Porous bed reactor with a moving solid matrix.

The modulus of $\overline{\mathbf{u}}_{rel}$ can be calculated as,

$$|\overline{\mathbf{u}}_{rel}| = |\overline{\mathbf{u}}_D - \mathbf{u}_S| = \sqrt{(\overline{u}_D - u_S)^2 + (\overline{v}_D - v_S)^2 + (\overline{w}_D - w_S)^2}. \tag{10}$$

One could also define a phase-volume based relative velocity as,

$$\overline{\mathbf{u}}^{\gamma}_{rel} = \langle \overline{\mathbf{u}} \rangle^i - \langle \mathbf{u} \rangle^s \tag{11}$$

and the relationship between these two relative velocities becomes,

$$\frac{\overline{\mathbf{u}}_{rel}}{\overline{\mathbf{u}}^{\gamma}_{rel}} = \left(\frac{\phi - (1-\phi)\frac{\langle \mathbf{u} \rangle^s}{\langle \overline{\mathbf{u}} \rangle^i}}{1 - \frac{\langle \mathbf{u} \rangle^s}{\langle \overline{\mathbf{u}} \rangle^i}} \right). \tag{12}$$

Although it is recognized that the drag between phases can be related to $\overline{\mathbf{u}}^{\gamma}_{rel}$, in the equations to follow, for simplicity, $\overline{\mathbf{u}}_{rel}$ will be used for characterizing the relative movement between phases. Further, for $\langle \mathbf{u} \rangle^s = 0$ the result $\overline{\mathbf{u}}_{rel} = \phi\, \overline{\mathbf{u}}^{\gamma}_{rel}$ is equivalent to $\overline{\mathbf{u}}_D = \phi \langle \overline{\mathbf{u}} \rangle^i$ and for $\langle \mathbf{u} \rangle^s / \langle \overline{\mathbf{u}} \rangle^i = 1$ one gets $\overline{\mathbf{u}}^{\gamma}_{rel} / \overline{\mathbf{u}}_{rel} = 0$ [26].

2.2. Macroscopic continuity equation

As previously commented, most of the equations to be shown below are already fully detailed in the literature so that only their final modeled form will be repeated.

The continuity of fluid mass reads:

$$\nabla . \rho_f \overline{\mathbf{u}}_D = 0. \tag{13}$$

Eq. (13) represents the macroscopic continuity equation for the gas. Regardless if the solid phase is moving, Eq. (13) holds for the fluid phase.

2.3. Macroscopic momentum equation

For a fixed bed, the momentum equation for macroscopic turbulent flow reads [25]:

$$\nabla \cdot \left(\rho_f \frac{\overline{\mathbf{u}}_D\, \overline{\mathbf{u}}_D}{\phi} \right) = -\nabla \left(\phi \langle \overline{p} \rangle^i \right) + \mu \nabla^2 \overline{\mathbf{u}}_D + \nabla \cdot \left(-\rho_f \phi \langle \overline{\mathbf{u}'\, \mathbf{u}'} \rangle^i \right) - \left[\frac{\mu \phi}{K} \overline{\mathbf{u}}_D + \frac{c_F \phi\, \rho_f |\overline{\mathbf{u}}_D|\, \overline{\mathbf{u}}_D}{\sqrt{K}} \right] \tag{14}$$

where the last two terms in Eq. (14) represent the Darcy and Forchheimer contributions. The symbol K is the porous medium permeability, $c_F = 0.55$ is the form drag coefficient, $\langle p \rangle^i$ is the intrinsic (fluid phase averaged) pressure of the fluid, ρ_f is the fluid density, μ represents the fluid viscosity.

Assuming that a model for the Macroscopic Reynolds Stresses $-\rho_f \phi \langle \overline{\mathbf{u}'\, \mathbf{u}'} \rangle^i$ is given by (see [25] for details),

$$-\rho_f \phi \langle \overline{\mathbf{u}'\, \mathbf{u}'} \rangle^i = \mu_{t_\phi} 2 \langle \overline{\mathbf{D}} \rangle^{\mathbf{v}} - \frac{2}{3} \phi \rho_f \langle k \rangle^i \mathbf{I} \tag{15}$$

with,

$$\langle \overline{\mathbf{D}} \rangle^v = \frac{1}{2} \left[\nabla \left(\phi \langle \overline{\mathbf{u}} \rangle^i \right) + \left[\nabla \left(\phi \langle \overline{\mathbf{u}} \rangle^i \right) \right]^T \right], \tag{16}$$

the momentum Eq. (14) reads after dropping body forces and some rearrangement,

$$\nabla \cdot \left(\rho_f \frac{\overline{\mathbf{u}}_D \overline{\mathbf{u}}_D}{\phi} \right) - \nabla \cdot \left\{ \left(\mu + \mu_{t_\phi} \right) \left[\nabla \overline{\mathbf{u}}_D + (\nabla \overline{\mathbf{u}}_D)^T \right] \right\} = -\nabla \left(\phi \langle \overline{p} \rangle^i \right) - \left[\frac{\mu \phi}{K} \overline{\mathbf{u}}_D + \frac{c_F \phi\, \rho_f |\overline{\mathbf{u}}_D|\, \overline{\mathbf{u}}_D}{\sqrt{K}} \right] \tag{17}$$

where

$$\mu_{t_\phi} = \rho_f\, c_\mu \frac{\langle k \rangle^{i^2}}{\langle \varepsilon \rangle^i}. \tag{18}$$

Note that in Eq. (17) a modified pressure is used that includes the last term in Eq. (15).

Assuming now that a relative movement between the two phases is described by Eq. (8), the previous momentum Eq. (17) reads now [26],

$$\nabla \cdot \left(\rho_f \frac{\overline{\mathbf{u}}_D \overline{\mathbf{u}}_D}{\phi} \right) - \nabla \cdot \left\{ \left(\mu + \mu_{t_\phi} \right) \left[\nabla \overline{\mathbf{u}}_D + (\nabla \overline{\mathbf{u}}_D)^T \right] \right\} = -\nabla \left(\phi \langle \overline{p} \rangle^i \right) - \underbrace{\left[\frac{\mu \phi}{K} \overline{\mathbf{u}}_{rel} + \frac{c_F\, \phi \rho_f |\overline{\mathbf{u}}_{rel}|\, \overline{\mathbf{u}}_{rel}}{\sqrt{K}} \right]}_{\text{Viscous and Form drags due to } \overline{\mathbf{u}}_{rel}}. \tag{19}$$

The last two terms in the above equation represent the drag caused by the difference in speed of the solid matrix and the flowing gas. When the two materials flow along with the same velocity, then fluid elements feel no extra forces caused by the porous matrix. Pressure head necessary to drive the flow is therefore less then that required to push the fluid through a fixed porous substrate.

2.4. Turbulence modeling

Turbulence is handled by a macroscopic form of the standard k-ε model (see [25] for details). A transport equation for $\langle k \rangle^i = \langle \overline{\mathbf{u}' \cdot \mathbf{u}'} \rangle^i / 2$ can be written as [26],

$$\nabla \cdot \left(\rho_f \overline{\mathbf{u}}_D \langle k \rangle^i \right) = \nabla \cdot \left[\left(\mu + \frac{\mu_{t_\phi}}{\sigma_k} \right) \nabla \left(\phi \langle k \rangle^i \right) \right] \underbrace{- \rho_f \langle \overline{\mathbf{u}'\, \mathbf{u}'} \rangle^i : \nabla \overline{\mathbf{u}}_D}_{P^i} + \underbrace{c_k\, \rho_f \frac{\phi \langle k \rangle^i |\overline{\mathbf{u}}_{rel}|}{\sqrt{K}}}_{G^i} - \rho_f \phi \langle \varepsilon \rangle^i \tag{20}$$

where $P^i = -\rho_f \langle \overline{\mathbf{u}'\,\mathbf{u}'} \rangle^i : \nabla \overline{\mathbf{u}}_D$ is the production rate of $\langle k \rangle^i$ due to gradients of $\overline{\mathbf{u}}_D$ and the generation rate due to the porous substrate, G^i, now depends on $|\overline{\mathbf{u}}_{rel}|$ and reads,

$$G^i = c_k \rho_f \phi \langle k \rangle^i |\overline{\mathbf{u}}_{rel}| / \sqrt{K}. \tag{21}$$

If there is no relative motion between the two phases, $\overline{\mathbf{u}}_{rel} = 0$, implying that no mean kinetic energy is transformed into turbulence by the action of porous substrate. In this case, G^i will be of null value.

A corresponding equation for $\langle \varepsilon \rangle^i = \mu \langle \overline{\nabla \mathbf{u}' : (\nabla \mathbf{u}')^T} \rangle^i / \rho_f$ reads,

$$\nabla \cdot \left(\rho_f \overline{\mathbf{u}}_D \langle \varepsilon \rangle^i \right) = \nabla \cdot \left[\left(\mu + \frac{\mu_{t_\phi}}{\sigma_\varepsilon} \right) \nabla \left(\phi \langle \varepsilon \rangle^i \right) \right] + c_1 \left(-\rho_f \langle \overline{\mathbf{u}'\,\mathbf{u}'} \rangle^i : \nabla \overline{\mathbf{u}}_D \right) \frac{\langle \varepsilon \rangle^i}{\langle k \rangle^i} + \underbrace{c_2\, c_k\, \rho_f \frac{\phi \langle k \rangle^i |\overline{\mathbf{u}}_{rel}|}{\sqrt{K}}}_{G^i} \frac{\langle \varepsilon \rangle^i}{\langle k \rangle^i} - c_2\, \rho_f \phi \frac{\langle \varepsilon \rangle^{i\,2}}{\langle k \rangle^i}. \tag{22}$$

3. Macroscopic heat transfer

Macroscopic energy equations are obtained for both fluid and solid phases by also applying time and volume average operators to the instantaneous local equations [33]. As in the flow case, volume integration is performed over a Representative Elementary Volume (REV). After including the heat released due to the combustion reaction, one gets for both phases:

$$\text{Gas}: \nabla \cdot (\rho_f\, c_{pf}\, \overline{\mathbf{u}}_D \langle \overline{T}_f \rangle^i) = \nabla \cdot \left\{ \mathbf{K}_{eff,f} \cdot \nabla \langle \overline{T}_f \rangle^i \right\} + h_i a_i \left(\langle \overline{T}_s \rangle^i - \langle \overline{T}_f \rangle^i \right) + \phi \Delta H\, S_{fu}, \tag{23}$$

$$\text{Solid}: \nabla \cdot (\rho_s\, c_{ps}\, \mathbf{u}_s \langle \overline{T}_s \rangle^i) = \nabla \cdot \left\{ \mathbf{K}_{eff,s} \cdot \nabla \langle \overline{T}_s \rangle^i \right\} - h_i a_i \left(\langle \overline{T}_s \rangle^i - \langle \overline{T}_f \rangle^i \right), \tag{24}$$

where, $a_i = A_i / V$ is the interfacial area per unit volume, h_i is the film coefficient for interfacial transport, $\mathbf{K}_{eff,f}$ and $\mathbf{K}_{eff,s}$ are the effective conductivity tensors for fluid and solid, respectively, given by,

$$\mathbf{K}_{eff,f} = \left\{ \overbrace{\phi\, k_f}^{conduction} \right\} \mathbf{I} + \underbrace{\mathbf{K}_{f,s}}_{\text{local conduction}} + \underbrace{\mathbf{K}_{disp}}_{\text{dispersion}} + \underbrace{\mathbf{K}_t + \mathbf{K}_{disp,t}}_{\text{turbulence}} \tag{25}$$

$$\mathbf{K}_{eff,s} = \left\{ \overbrace{(1-\phi)[k_s + \frac{16\sigma \left(\langle \overline{T} \rangle^i \right)^3}{3\beta_r}]}^{conduction} \right\} \mathbf{I} + \underbrace{\mathbf{K}_{s,f}}_{\text{local conduction}} \quad . \tag{26}$$

In Eqs. (23)–(26), $\mathbf{I}$ is the unit tensor, ΔH is the heat of combustion, β_r is the extinction coefficient, σ is the Stephan–Boltzman constant [5.66961×10^{-8} W/m^{2}K^4] and S_{fu} is the rate of fuel consumption, to be commented upon later. All mechanisms contributing to heat transfer within the medium, together with turbulence and radiation, are included as they impact on temperature distributions within the domain. Further, such distinct contributions of various mechanisms are the outcome of the application of gradient type diffusion models, in the form [33]:

$$\text{Turbulent heat flux}: -\left(\rho\, c_p \right)_f \left(\phi\ \overline{\langle \mathbf{u}' \rangle^i \langle T_f' \rangle^i} \right) = \mathbf{K}_t \cdot \nabla \langle\, \overline{T}_f \rangle^i \quad . \tag{27}$$

$$\text{Thermal dispersion}: -\left(\rho\, c_p \right)_f \left(\phi\ \langle {}^i\mathbf{u}'\, {}^i \overline{T}_f \rangle^i \right) = \mathbf{K}_{disp} \cdot \nabla \langle\, \overline{T}_f \rangle^i \, . \tag{28}$$

$$\text{Turbulent thermal dispersion}: -\left(\rho\, c_p \right)_f \left(\phi\ \langle {}^i\overline{\mathbf{u}'^i T_f'} \rangle^i \right) = \mathbf{K}_{disp,t} \cdot \nabla \langle\, \overline{T}_f \rangle^i \, . \tag{29}$$

$$\text{Local conduction}: \nabla \cdot \left[\frac{1}{V} \int_{A_i} \mathbf{n}_i\, k_f\, \overline{T}_f\, dA \right] = \mathbf{K}_{f,s} \cdot \nabla \langle\, \overline{T}_s \rangle^i \quad . \qquad -\nabla \cdot \left[\frac{1}{V} \int_{A_i} \mathbf{n}_i\, k_s \overline{T}_s\, dA \right] = \mathbf{K}_{s,f} \cdot \nabla \langle\, \overline{T}_f \rangle^i \tag{30}$$

3.1. Interstitial heat transfer coefficient

In Eqs. (23) and (24) the heat transferred between the two phases was modeled by means of a film coefficient, h_i, such that:

$$h_i a_i \left(\langle \overline{T}_s \rangle^i - \langle \overline{T}_f \rangle^i \right) = \frac{1}{\Delta V} \int_{A_i} \mathbf{n}_i \cdot k_f \nabla\, \overline{T}_f dA = \frac{1}{\Delta V} \int_{A_i} \mathbf{n}_i \cdot k_s \nabla\, \overline{T}_s dA \, . \tag{31}$$

where, A_i is the interfacial area between the two phases and a_i, as mentioned above, is the interfacial area per unit volume or $a_i = A_i / \Delta V$. In foam-like or cellular media, the high values of a_i make them attractive for transferring thermal energy via conduction through the solid followed by convection to a fluid stream.

A numerical correlation for the interfacial convective heat transfer coefficient was proposed by Kuwahara et al. [34] for laminar flow as:

$$\frac{h_i D}{k_f} = \left(1 + \frac{4(1-\phi)}{\phi} \right) + \frac{1}{2} (1-\phi)^{1/2}\, Re_D\, Pr^{1/3}, \text{valid for } 0.2 < \phi < 0.9 \, . \tag{32}$$

For turbulent flow, the following expression was proposed in Saito and de Lemos [33]:

$$\frac{h_i D}{k_f} = 0.08 \left(\frac{Re_D}{\phi} \right)^{0.8} Pr^{1/3}; \text{for } 1.0 \times 10^4 < \frac{Re_D}{\phi} < 2.0 \times 10^7, \text{valid for } 0.2 < \phi < 0.9 \, . \tag{33}$$

The interstitial heat transfer coefficient h_i is calculated by correlations (32) and (33) for laminar and turbulent flow, respectively. However, since the relative movement between phases is seen as the promoter of convective heat transport from the fluid to the solid, or vice-versa, a relative Reynolds number defined as,

$$Re_D = \frac{\rho |\overline{\mathbf{u}}_{rel}| D}{\mu} \tag{34}$$

is used in the correlations (32) and (33) instead of a Reynolds number based on the absolute velocity of the fluid phase. Accordingly, when the solid phase velocity approaches the fluid velocity, it is assumed here that the only mechanism for transferring heat between phases is conduction.

4. Macroscopic combustion model

In this work, the gas phase is assumed to be composed by a premixture of air and gaseous fuel that undergoes combustion while the solid matrix moves along with the gases. For analyzing such system, the equation set above is complemented with a transport equation for the fuel and a kinetics model for the burning process [28].

4.1. Mass transport for fuel

Transport equation for the fuel reads,

$$\nabla \cdot \left(\rho_f \overline{\mathbf{u}}_D \langle\, \overline{m}_{fu} \rangle^i \right) = \nabla \cdot \rho_f \mathbf{D}_{eff} \cdot \nabla \left(\phi \langle\, \overline{m}_{fu} \rangle^i \right) - \phi\, S_{fu} \tag{35}$$

where $\langle \bar{m}_{fu} \rangle^i$ is the mass fraction for the fuel. The effective mass transport tensor, $\mathbf{D}_{eff}$, is defined as:

$$\mathbf{D}_{eff} = \underbrace{\mathbf{D}_{disp}}_{dispersion} + \overbrace{\mathbf{D}_{diff}}^{diffusion} + \underbrace{\mathbf{D}_t + \mathbf{D}_{disp,t}}_{turbulence} = \mathbf{D}_{disp} + \frac{1}{\rho_f}\left(\frac{\mu_\phi}{Sc_\ell} + \frac{\mu_{t_\varphi}}{Sc_{\ell,t}}\right)\mathbf{I}$$
$$= \mathbf{D}_{disp} + \frac{1}{\rho_f}\left(\frac{\mu_{\phi,eff}}{Sc_{\ell,eff}}\right)\mathbf{I} \tag{36}$$

where Sc_ℓ and $Sc_{\ell,t}$ are the laminar and turbulent Schmidt numbers for species ℓ, respectively, and "*eff*" denotes an effective value. The dispersion tensor is defined such that,

$$-\rho_f \phi \langle^i \bar{\mathbf{u}}^i \bar{m}_{\mathrm{fu}} \rangle^{\mathrm{i}} = \rho_f \mathbf{D}_{disp} \cdot \nabla\left(\phi \langle m_{fu} \rangle^i\right). \tag{37}$$

4.2. Simple chemistry

In this work, for simplicity, it is assumed that the exothermic reaction is instantaneous and occurs in a single step, or say, it is kinetic-controlled, a condition that for combustion of a mixture air/methane is represented by the chemical reaction [12–14],

$$CH_4 + 2(1+\Psi)(O_2 + 3.76N_2) \rightarrow CO_2 + 2H_2O + 2\Psi O_2 + 7.52(1+\Psi)N_2. \tag{38}$$

For the case of *N*-heptane, reference [14] presents a similar equation, which reads,

$$C_7H_{16} + 11(1+\Psi)(O_2 + 3.76N_2) \rightarrow 7CO_2 + 8H_2O + 11\Psi O_2 + 41.36(1+\Psi)N_2 \tag{39}$$

and for Octane, one has,

$$C_8H_{18} + 12.5(1+\Psi)(O_2 + 3.76N_2) \rightarrow 8CO_2 + 9H_2O + 12.5\Psi O_2 + 47(1+\Psi)N_2. \tag{40}$$

In the above chemical reactions, Ψ is the excess air in the reactant stream at the inlet of the porous bed. A general expression for them can be derived as,

$$C_nH_{2m} + \left(n + \frac{m}{2}\right)(1+\Psi)(O_2 + 3.76N_2) \rightarrow nCO_2 + mH_2O + \left(n + \frac{m}{2}\right)\Psi O_2 + \left(n + \frac{m}{2}\right)3.76(1+\Psi)N_2 \tag{41}$$

where the coefficients n and m can be found in Table 1. Eq. (41) is here assumed to hold for the particular examples given in the table. Further, for the stechiometric ratio, $\Psi = 0$.

The local instantaneous rate of fuel consumption over the total volume (fluid plus solid) was determined by a one step Arrhenius reaction [35, 36], given by,

$$S_{fu} = \rho_f^2 A \langle m_{fu} \rangle^i \langle m_{ox} \rangle^i \; e^{-E/R\langle \bar{T} \rangle^i} \tag{42}$$

where $\langle m_{fu} \rangle^i$ and $\langle m_{ox} \rangle^i$ are the local instantaneous mass fractions for the fuel and oxidant, respectively. Also, in Eq. (42) A is the pre-exponential factor and E is the activation energy, where numerical values for these parameters depend on the fuel considered [35].

Before presenting the results, a word on the use of Eq. (42) seems timely. Here, for simplicity, Eq. (42) is assumed to hold for turbulent flow in porous media, which might not be the case when calculating turbulent free flame properties. For a discussion on possible extensions of Eq. (42) to account for additional turbulent flow effects, see [29].

Further, density ρ_f in the above equations is determined from the perfect gas equation for a mixture of perfect gases:

$$\rho_f = \frac{P_o}{RT_f \sum_1^\ell \frac{m_\ell}{M_\ell}} \tag{43}$$

where P_o is a reference pressure, R is the universal gas constant [8.134 J/(mol.K)] and M_ℓ is the molecular weight of species ℓ.

Table 1
Coefficients in the general combustion Eq. (41).

Gas	n	m	(n + m/2)	(n + m/2) × 3.76
Methane	1	2	2	7.52
N-heptane	7	8	11	41.36
Octane	8	9	12.5	47

5. Sample results

We present here sample results for the plug flow formed by the moving bed and flowing gas depicted in the system of Fig. 1. The air/methane mixture enters the moving bed reactor and undergoes combustion consuming fuel at a rate given by Eq. (42). Density is updated using Eq. (43). Here, we considered that the gas phase flows from left to right and leaves the porous reactor at $x = L$. The exact location of the flame front, if combustion takes place, is the sole outcome of the iterative process and no artificial numerical gimmick is implemented. For a discussion on the numerics implemented in solving the above equation, the reader is urged to see [28].

Fig. 2*a* presents results for the axial non-dimensional fluid and solid temperatures taken at the middle height of the channel ($y = H/2$) for distinct values of the velocity slip ratio u_s/u_D. Temperatures were non-dimensionalized using the expression,

$$\Theta_{s,f} = \frac{T_{s,f} - T_{\min}}{T_{\max} - T_{\min}} \tag{44}$$

where "max" and "min" refer to values in the entire computational domain of Fig. 1. As the solid phase moves faster, approaching the speed of the fluid stream, a longer entry length is necessary for thermal equilibrium to be achieved since the relative velocity between phases is reduced and, consequently, less intense is the exchange of heat between phases. Also, the flame front, indicated here by the position where the gas phase reaches its maximum value, is moved forward, towards the end of the reactor. The figure also indicates that for higher values of u_s final equilibrium temperatures are lower. Keeping the same mass flow rate of the incoming fuel, the amount of generated heat is the same, regardless of the speed of the solid. As a result, a higher solid speed will yield a lower solid temperature at the exit, bring down the fluid temperature by means of the exchange of heat between phases.

Finally, Fig. 2*b* shows results for the statistical filed in terms of the non-dimensional turbulence kinetic energy $\langle k \rangle^v / u_{in}^2$. For a flat velocity profile quickly formed inside the porous reactor, production rates of turbulence kinetic energy are mostly due to the G^i-term that is described by the model of Eq. (21). With increasing of the ratio u_s/u_D, the relative velocity between phases is reduced, which, in turn, reduces the generation of turbulence inside the medium. For the parameters here employed and for $u_s/u_D > 0.25$, the flow leaves the reactor at x/L=1 without undergoing combustion. Further, as the solid speed increases, the amount of mean mechanical energy converted into turbulence is reduced.

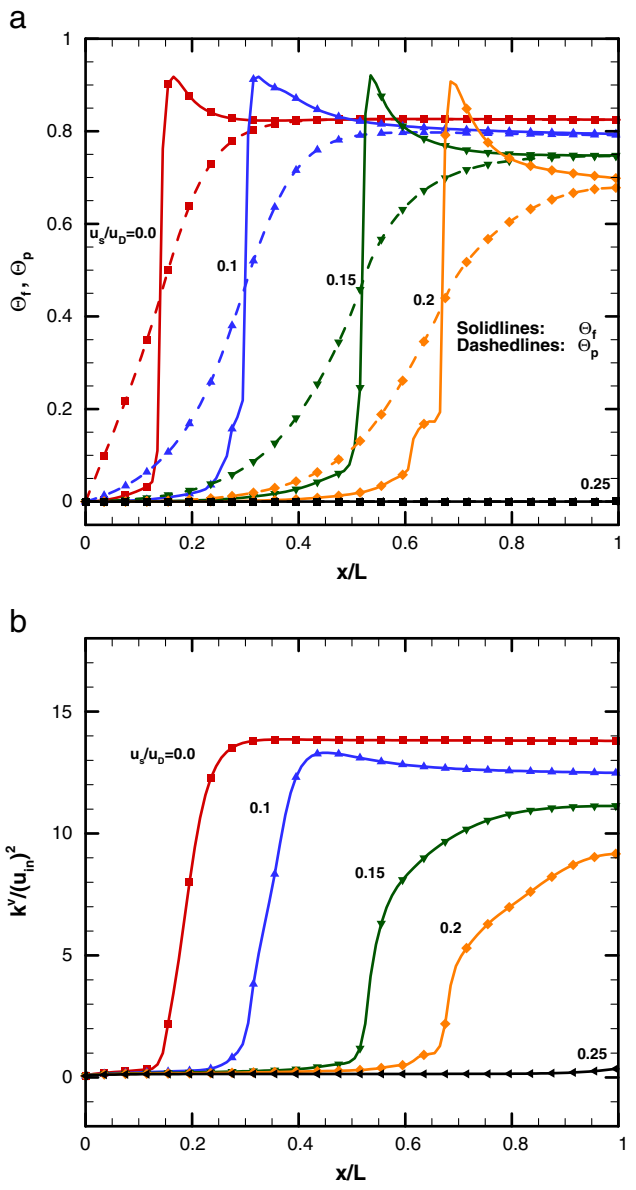

Fig. 2. Effect of velocity slip ratio u_s/u_D at $y = H/2$: *a*) nondimensional axial temperatures and *b*) turbulent kinetic energy.

6. Conclusions

This paper presents a proposal for a full two-energy equation allowing for movement of the porous bed and turbulent combustion of the gas stream. Fuel consumption rate is expressed by the kinetic controlled one-step Arrhenius expression, which contains products of mass fraction of fuel and oxidant. Preliminary testing results for a porous reactor with a moving bed and co-flowing gas indicates that the flame front moves forward as the relative phase velocity is reduced. In addition, the level of turbulence kinetic energy is reduced as less generation of k is obtained for higher values of the solid velocity.

Acknowledgments

The authors would like to express their gratitude to CNPq, CAPES and FAPESP, funding agencies in Brazil, for their invaluable support during the course of this research endeavor.

References

[1] R. Henda, D.J. Falcioni, Modeling of heat transfer in a moving packed bed: case of the preheater in nickel carbonyl process, Journal of Applied Mechanics 73 (2006) 47–53.
[2] M.S. Valipour, Y. Saboohi, Modeling of multiple noncatalytic gas–solid reactions in a moving bed of porous pellets based on finite volume method, Heat and Mass Transfer 43 (9) (2007) 881–894.
[3] J.A. Almendros-Ibáñez, A. Soria-Verdugo, U. Ruiz-Rivas, D. Santana, Solid conduction effects and design criteria in moving bed heat exchangers, Applied Thermal Engineering 31 (2011) 1200–1207.
[4] C. Ryu, Y.B. Yang, A. Khor, N.E. Yates, V.N. Sharifi, J. Swithenbank, Effect of fuel properties on biomass combustion: part i. experiments—fuel type, equivalence ratio and particle size, Fuel 85 (2006) 1039–1046.
[5] C. Boman, A. Nordin, L. Thaning, Effects of increased biomass pellet combustion on ambient air quality in residential areas — a parametric dispersion modeling study, Biomass and Bioenergy 24 (2003) 465–474.
[6] T. Shimizu, J. Han, S. Choi, L. Kim, H. Kim, Fluidized-bed combustion characteristics of cedar pellets by using an alternative bed material, Energy and Fuels 20 (2006) 2737–2742.
[7] T.K. Kayal, M. Chakravarty, Mathematical modeling of continuous updraft gasification of bundled jute stick — a low ash content woody biomass, Bioresource Technology 49 (1) (1994) 61–73.
[8] A. Rogel, J. Aguillón, The 2D Eulerian approach of entrained flow and temperature in a biomass stratified downdraft gasifier, American Journal of Applied Sciences 3 (10) (2006) 2068–2075.
[9] T. Nussbaumer, Combustion and co-combustion of biomass: fundamentals technologies, and primary measures for emission reduction, Energy and Fuels 17 (2003) 1510–1521.
[10] J.R. Howell, M.J. Hall, J.L. Ellzey, Combustion of hydrocarbon fuels within porous inert media, Progress in Energy and Combustion Science 22 (2) (1996) 121–145.
[11] M.R. Henneke, J.L. Ellzey, Modeling of filtration combustion in a packed bed, Combustion and Flame 117 (4) (1999) 832–840.
[12] A.A. Mohamad, S. Ramadhyani, R. Viskanta, Modeling of combustion and heat-transfer in a packed-bed with embedded coolant tubes, International Journal Heat Mass Transfer 37 (8) (1994) 1181–1191.
[13] I. Malico, J.C.F. Pereira, Numerical predictions of porous burners with integrated heat exchanger for household applications, Journal of Porous Media 2 (2) (1999) 1532–162.
[14] A.A. Mohamad, R. Viskanta, S. Ramadhyani, Numerical prediction of combustion and heat transfer in a packed bed with embedded coolant tubes, Combinatorial Science and Tecnology 96 (1994) 387–407.
[15] Y.-T. Yang, M.-L. Hwang, Numerical simulation of turbulent fluid flow and heat transfer characteristics in a rectangular porous channel with periodically spaced heated blocks, Numerical Heat Transfer, Part A: Applications 54 (8) (2008) 819–836.
[16] S. Wood, A.T. Harries, Porous burners for lean-burn applications, Progress in Energy and Combustion Science 34 (2008) 667–684.
[17] M. Abdul Mujeebu, M.Z. Abdullah, M.Z. Abu Bakar, A.A. Mohamad, M.K. Abdullaha, A review of investigations on liquid fuel combustion in porous inert media, Progress in Energy and Combustion Science 35 (2009) 216–230.
[18] J. Zhang, C. Zhu, Simulation of swirling turbulent flow and combustion in a combustor, Numerical Heat Transfer; Part A: Applications 55 (5) (2009) 448–46.
[19] M.P. Raju, J.S. T'ien, Development of direct multifrontal solvers for combustion problems, Numerical Heat Transfer Part B: Fundamentals 53 (3) (2008) 189–205.
[20] M.J.S. de Lemos, R.A. Silva, Turbulent flow over a layer of a highly permeable medium simulated with a diffusion-jump model for the interface, International Journal of Heat and Mass Transfer 49 (3–4) (2006) 546–556.
[21] E.J. Braga, M.J.S. de Lemos, Laminar natural convection in cavities filled with circular and square rods, International Communications in Heat and Mass Transfer 32 (10) (2005) 1289–1297.
[22] M.B. Saito, M.J.S. de Lemos, Interfacial heat transfer coefficient for non-equilibrium convective transport in porous media, International Communications in Heat and Mass Transfer 32 (5) (2005) 666–677.
[23] M.J.S. de Lemos, F.T. Dorea, Simulation of a turbulent impinging jet into a layer of porous material using a two-energy equation model, Numerical Heat Transfer; Part A: Applications 59 (l0) (2011) 769–798.
[24] C. Fischer, M.J.S. de Lemos, A turbulent impinging jet on a plate covered with a porous layer, Numerical Heat Transfer; Part A: Applications 58 (6) (2010) 429–456.
[25] M.J.S. de Lemos, Turbulence in porous media, Modeling and Applications, Elsevier, Amsterdam, 2006, p. 384, (ISBN: 0-08-044491-1).
[26] M.J.S. de Lemos, Turbulent kinetic energy in a moving porous bed, International Communications in Heat and Mass Transfer 35 (2008) 1049–1053.
[27] M.J.S. de Lemos, M.B. Saito, Computation of turbulent heat transfer in a moving porous bed using a macroscopic two-energy equation model, International Communications in Heat and Mass Transfer 35 (2008) 1262–1266.
[28] M.J.S. de Lemos, Numerical simulation of turbulent combustion in porous materials, International Communications in Heat and Mass Transfer 36 (2009) 996–1001.
[29] M.J.S. de Lemos, Analysis of turbulent combustion in inert porous media, International Communications of Heat and Mass Transfer 37 (4) (2010) 331–336.
[30] J.C. Slattery, Flow of viscoelastic fluids through porous media, A.I.Ch.E.J. 13 (1967) 1066–1071.

[31] S. Whitaker, Advances in theory of fluid motion in porous media, Industrial Engineering Chemistry 61 (1969) 14–28.
[32] W.G. Gray, P.C.Y. Lee, On the theorems for local volume averaging of multiphase system, International Journal .of Multiphase Flow 3 (1977) 333–340.
[33] M.B. Saito, M.J.S. de Lemos, A correlation for interfacial heat transfer coefficient for turbulent flow over an array of square rods, Journal of Heat Transfer 128 (2006) 444–452.
[34] F. Kuwahara, M. Shirota, A. Nakayama, A numerical study of interfacial convective heat transfer coefficient in two-energy equation model for convection in porous media, International Journal of Heat Mass Transfer 44 (2001) 1153–1159.
[35] S.R. Turns, S.R. Turns, An introduction to combustion: concepts and applications, An Introduction to Combustion: Concepts and Applications, McGraw-Hill, New-York, 1996.
[36] K.K. Kuo, Principles of Combustion, New York, John Wiley and Sons, 1996.